Manuscript ID: CY-ART-05-2019-000999

Drastic change in selectivity caused by addition of oxygen to the hydrogen stream for the hydrogenation of nitrite in water over a supported platinum catalyst

Jun Hirayama,[a] Kei-ichiro Yasuda,[b] Sayaka Misu,[b] Ryoichi Otomo[a] and Yuichi Kamiya[*a]

[a]*Faculty of Environmental Earth Science, Hokkaido University, Nishi 5, Kita 10, Kita-ku, Sapporo 060-0810, Japan*

[b]*Graduate School of Environmental Science, Hokkaido University, Nishi 5, Kita 10, Kita-ku, Sapporo 060-0810, Japan*

*Corresponding author

Yuichi Kamiya

E-mail: kamiya@ees.hokudai.ac.jp, Tel/Fax:+81-11-706-2217

Abstract: In the present study, we investigated the influence of the addition of O_2 to the H_2 reactant stream during the hydrogenation of NO_2^- in water on the catalytic performances of Al_2O_3-supported precious metal catalysts including Pd, Pt, Ir, Rh, and Ru with 0.3 mmol g^{-1} of the metal. Pd/Al_2O_3 showed high selectivity for N_2 irrespective of the presence and absence of O_2, and Rh and Ru/Al_2O_3 were inactive towards the hydrogenation of NO_2^- even in the absence of O_2. In contrast, while Pt/Al_2O_3 showed high selectivity for NH_3 (90%) in the absence of O_2 (P_{H2} = 0.2 atm and P_{O2} = 0 atm), the product drastically changed to N_2 with 93% selectivity when O_2 was added (P_{H2} = 0.2 atm and P_{O2} = 0.1 atm). Since Pt/Al_2O_3 was completely inactive towards the oxidation of NH_3 with O_2 in water under the reaction conditions, oxidative decomposition of the formed NH_3 was not the reason for the high selectivity for N_2 in the presence of O_2. Kinetic analysis of the reaction in the absence and presence of O_2 and studies on the effects of the Pt size suggested that hydrogen atoms activated on the Pt particles were mainly consumed by O_2 upon H_2O formation in the presence of O_2. We concluded that the inactivation of the Pt sites active for NH_3 formation and furthermore the change in the function of the sites to N_2 formation caused by the O_2 addition lead to the drastic change in the selectivity from NH_3 to N_2 in the presence of O_2.

1. Introduction

Selective hydrogenations over supported metal catalysts have been extensively studied since the discovery of the Lindlar catalyst for the hydrogenation of alkynes[1] because it is invaluable for the synthesis of various chemicals[2–4] as well as environmental purification.[5–10] A research goal in hydrogenation is to achieve high selectivity by optimizing the reaction conditions[11–13] in conjunction with catalyst design, wherein scientists search for the best combination of metal and support,[14–17] the addition of promoters,[18–21] and applying special preparation techniques and conditions. In most hydrogenation reactions involving alkynes, dienes, esters, arenes, nitriles, nitros, amides, and so on, successive hydrogenation of partially hydrogenated products should be suppressed to achieve high selectivity by preventing the product from re-adsorption or facilitating desorption from the active site.

Another type of selective hydrogenation involves the formation of two or more possible products through parallel reactions. Since the reaction pathways for parallel hydrogenation are quite different from those of successive one, different approaches are required to achieve high selectivity. Hydrogenation of nitrite (NO_2^-) over precious metal catalysts in water, in which NH_3 and N_2 are possibly formed, is an example of parallel hydrogenation.[22] Scheme 1 shows a possible pathway for this reaction.[23,24] In the

course of the reaction, atomic nitrogen adsorbed on the catalyst, which is denoted as N_{ad}, is formed as an intermediate. The reaction of N_{ad} on the catalyst determines the products. NH_3 likely forms when the concentration of adsorbed hydrogen (H_{ad}) on the catalyst is high since the reaction of N_{ad} with H_{ad} affords NH_3. On the other hand, two N_{ad} are necessary to form N_2, and thus, a high concentration of H_{ad} may decrease the amount of N_{ad}, preventing N_2 formation. In other words, the surface concentrations of N_{ad} and H_{ad} could determine the selectivity of the reaction.

In the present study, we investigated the influence of O_2 in the H_2 reactant stream on the catalytic performances of supported precious metal catalysts for hydrogenation of NO_2^- in water and found a drastic change in the products from NH_3 to N_2 over Pt/Al_2O_3 in the presence of O_2. The hydrogenation of NO_2^- in the presence of O_2 has an advantage in environmental purification because the selective reduction of NO_2^- to N_2 can contribute to purification of groundwater polluted with NO_2^- as well as NO_3^-, which is now a serious global problem.[25–27]

2. Experimental

2.1. Chemicals

$H_2PtCl_6 \cdot 6H_2O$ (metal purity, 99.9 mol%), $RuCl_3 \cdot nH_2O$ (metal purity, 99.9mol%), $PdCl_2$ (metal purity, 99.0 mol%), and KNO_2 (95 wt. %) were purchased from Wako Pure Chemical Industries. $Na_3RhCl_6 \cdot nH_2O$ (metal purity, 80 mol%) and $Na_2IrCl_6 \cdot 6H_2O$ (metal purity, 97 mol%) were obtained from Kanto Chemical Co., Inc. All chemicals were used as received without further purification.

2.2. Preparation of catalyst

Alumina-supported precious metal catalysts were prepared by using incipient wetness impregnation. A powder of γ-Al_2O_3 (AEROSIL®, Alu C) was treated in air at 523 K for 4 h before use. An aqueous solution of the metal salt was dropped onto the Al_2O_3, and then the resulting wet solid was dried in air at 373 K overnight, followed by calcination in air at 523 K for 3 h (rate of temperature increase, 10 K min^{-1}). Just before the catalytic reactions were performed, the catalyst was reduced with H_2 in a flow reactor. The temperature was increased at a rate of 10 K min^{-1} under H_2 flow and was kept at 623 K for 1 h. After the temperature was decreased to room temperature, the catalyst was quickly transferred to the reactor for the catalytic hydrogenation of NO_2^-. The loading amount of metal was fixed at 0.3 mmol g^{-1}. The obtained catalysts are denoted as *M*/Al_2O_3 (*M*: Pd, Pt, Ir, Rh, and Ru).

To investigate the effect of Pt particle size on the hydrogenation of NO_2^- over Pt/Al_2O_3,

Pt/Al_2O_3 with 0.15 and 0.62 mmol g^{-1} of Pt loadings were prepared using the procedure mentioned above with different amounts of the aqueous solution of H_2PtCl_6 dropped on the Al_2O_3. The sizes of the Pt particles were estimated from chemisorption amount of CO at 323 K to be 3.6, 4.1, and 6.7 nm for Pt loadings of 0.15, 0.30, and 0.62 mmol g^{-1}, respectively.

2.3. Characterization

Adsorption–desorption isotherms of N_2 at 77 K were acquired on a Belsorp-mini instrument (BEL Japan Inc.) after the samples were pretreated at 473 K in a N_2 flow for 1 h. Specific surface areas were estimated by using the Brunauer–Emmett–Teller (BET) equation applied to the adsorption isotherms of N_2. The average sizes of metal particles on Al_2O_3 were estimated by using transmission electron microscopy (TEM) using a JEM-2100F (JEOL), and a CO adsorption technique, which were carried out at 323 K by using a BEL CAT instrument (BEL Japan Inc.). Prior to the CO adsorption experiment, the sample (0.1 g) was reduced with H_2 at 623 K for 1 h.

Physical properties of the catalysts are summarized in Table S1 (Electric Supplementary Information, ESI). TEM images of the catalysts used for estimation of the particle sizes are shown in Fig. S1.

2.4. Catalytic reactions

Catalytic hydrogenation of NO_2^- in water was carried out in a semi-batch reactor at 298 K (Fig. S2). The reaction mixture (100 cm^3, KNO_2, 1.0 mmol dm^{-3}) containing catalyst powder was sparged with a stream of Ar (30 cm^3 min^{-1}) for 30 min. Then the gas was switched to the reactant gas containing H_2 to start the reaction. In case of the normal reaction conditions without O_2, a gas mixture composed of H_2, CO_2, and Ar with partial pressures (P_x) of 0.2, 0.3, and 0.5 atm, respectively, was flowed into the reaction solution. This condition is denoted as **NO_2^--H_2**. On the other hand, a gas mixture composed of H_2, CO_2, Ar and O_2 with partial pressures of 0.2, 0.3, 0.4 and 0.1 atm, respectively, was used for the reaction in the presence of O_2 (**NO_2^--H_2-O_2**). The total flow rate was 100 cm^3 min^{-1} for both reaction conditions. A small portion of the reaction mixture was periodically withdrawn, and the concentrations of NO_2^-, NO_3^-, and NH_3 in the solution were determined by using two ion chromatographs (IC2001, Tosoh). A column containing an anion-exchange resin (TSK gel Super IC-AZ, Tosoh) and an aqueous solution of $NaHCO_3$ (2.9 mmol dm^{-3}) and Na_2CO_3 (3.1 mmol dm^{-3}) were used as stationary and mobile phases, respectively, for anion analysis. For cation analysis, a column containing a cation-exchange resin (TSK gel IC-Cation 1/2 HR, Tosoh) and an aqueous solution of methanesulfonic acid (2.2 mmol dm^{-3}) and 18-crown-6 (1.0 mmol dm^{-3}) were used as stationary and mobile phases, respectively. The gas was analyzed using a gas chromatograph (Shimadzu Co., GC-8A, Shimazu) equipped with a thermal conductivity detector (TCD) and a molecular sieves column.

No gaseous products other than N_2 were detected under either reaction conditions regardless of the catalyst used.

The reaction rate for NO_2^- consumption (decomposition) was estimated from the data where the decrease in the concentration of NO_2^- occurred almost linearly with the reaction time. The selectivities for NH_3 and NO_3^- were calculated by using Eq. (1).

$$\text{Selectivity for } NH_3 \ (or\ NO_3^-)[\%] = \frac{\text{Concentration of formed } NH_3 \ (or\ NO_3^-)}{\text{Concentration of consumed } NO_2^-} \times 100 \qquad (1)$$

The selectivity for N_2 was calculated by subtracting the selectivities for NH_3 and NO_3^- from 100%.

The catalytic reaction of O_2 with H_2, i.e., a H_2O formation reaction, in water over M/Al_2O_3 in the absence of NO_2^- was performed similar to that for the catalytic hydrogenation of NO_2^-.

3. Results and discussion

3.1. Effects of O_2 addition on the hydrogenation of NO_2^- in water

Figure 1 shows catalytic performances of Al_2O_3-supported precious metal catalysts in the absence (**NO_2^--H_2**) and presence of O_2 (**NO_2^--H_2-O_2**). Although Rh/Al_2O_3 and Ru/Al_2O_3 were basically inactive, Pd/Al_2O_3 and Pt/Al_2O_3 showed activity for the

hydrogenation of NO_2^- (Fig. 1(a)). However, the responses to the addition of O_2 depended on the catalysts. Pd/Al_2O_3 gave mainly N_2 irrespective of the presence or absence of O_2 (Fig. 1(b)). In contrast, Pt/Al_2O_3 showed a drastic change in the product by the addition of O_2. Although NH_3 was selectively formed over Pt/Al_2O_3 in $\mathbf{NO_2^-\text{-}H_2}$, N_2 became the dominant product in $\mathbf{NO_2^-\text{-}H_2\text{-}O_2}$. The product over Ir/Al_2O_3 changed in the presence of O_2, but the change was not so significant, and the activity was negligibly low in the presence of O_2.

As mentioned above, only Pd/Al_2O_3 and Pt/Al_2O_3 showed decent activity, but the activity of the former significantly decreased in the presence of O_2. It was presumed that this activity loss over Pd/Al_2O_3 was caused by progression of the H_2O formation reaction in the presence of O_2 in parallel with the hydrogenation of NO_2^-. To confirm this, we carried out the reaction of O_2 with H_2 in water over M/Al_2O_3 in the absence of NO_2^- (Figure 2). As Fig. 2 shows, Pd/Al_2O_3 was quite active for the H_2O formation reaction. On the other hand, Pt/Al_2O_3 showed about three times less activity than Pd/Al_2O_3 did. The low activity of Pt/Al_2O_3 for the H_2O formation reaction explains the relatively high activity for the hydrogenation of NO_2^- in $\mathbf{NO_2^-\text{-}H_2\text{-}O_2}$.

Since Pt/Al_2O_3 exhibited good catalytic performance in the hydrogenation of NO_2^- in the presence of O_2, we further investigated the catalytic performance in detail. Figure 3

shows the changes in selectivity for NH_3 during NO_2^- conversion in **NO_2^--H_2** and **NO_2^--H_2-O_2** over Pt/Al_2O_3. For **NO_2^--H_2**, the selectivity for NH_3 was around 50% up to a conversion of 60% and then increased to 91% at 100% conversion. As the conversion increased, the concentration of NO_2^- in the reaction solution decreased. Thus, it is thought that the surface concentration of N_{ad} is low at such high conversions and that of H_{ad} is high, resulting in the increase in the selectivity for NH_3 with an increase in the conversion. In contrast, the selectivity for NH_3 was low at all conversions in **NO_2^--H_2-O_2**.

We thought that the progression of oxidative decomposition of formed NH_3 with O_2 over Pt/Al_2O_3 caused the low selectivity for NH_3 in the presence of O_2. In order to confirm this, we conducted oxidative decomposition of NH_3 in water over Pt/Al_2O_3 under the conditions similar to that of **NO_2^--H_2-O_2** but in the absence of NO_2^- (Fig. S3(A)). However, Pt/Al_2O_3 was completely inactive for the reaction. Furthermore, Pt/Al_2O_3 showed no activity for the oxidative decomposition of NH_3 even in the absence of H_2 (Fig. S3(B)). Thus, we believe that the surface concentration of H_{ad} remains constantly at a moderate level on Pt/Al_2O_3 under the reaction conditions for **NO_2^--H_2-O_2** owing to the consumption of H_{ad} by the reaction with O_2. Therefore, the selectivity for NH_3 was low for the hydrogenation of NO_2^- in the presence of O_2, whereas that for N_2 was high.

3.2. Reaction conditions developing the selectivity change

As discussed in section 3.1, the product over Pt/Al_2O_3 drastically changed from NH_3 to N_2 when O_2 was added. To determine the partial pressure of O_2 giving rise to the change in selectivity, we investigated the influence of the partial pressure of O_2 on the hydrogenation of NO_2^- over Pt/Al_2O_3 with the P_{H2} fixed at 0.1 atm (Fig. 4). The selectivity for N_2 increased with an increase in the P_{O2} and reached a maximum when P_{O2} was 0.05 atm, whereas the NO_2^- decomposition rate decreased with an increase in the P_{O2}. In addition to the sharp drop in the NO_2^- decomposition rate, NO_3^- appeared at high P_{O2}. In fact, we confirmed that the oxidation of NO_2^- with O_2 proceeded over Pt/Al_2O_3 without H_2 (Figure S4). Therefore, it was concluded that the optimal P_{O2} was 0.05 atm, which corresponded to half of the H_2 partial pressure.

3.3 Kinetic study and mechanism of the selectivity change caused by the addition of O_2

To further understand what occurred on Pt/Al_2O_3 in the presence of O_2, we performed a kinetic study in the absence and presence of O_2. To estimate the reaction orders with respect to NO_2^- and H_2, we plotted the logarithms of the NO_2^--decomposition rate for the hydrogenation of NO_2^- over Pt/Al_2O_3 as a function of the logarithms of the initial NO_2^- concentrations ($[NO_2^-]_0$) in the

range of 0.5–2.0 mmol dm^{-3} and P_{H2} in the range of 0.1–0.4 atm (Figure S5). From the slopes of the plots, the reaction orders for the reactions in the absence and presence of O_2 were estimated to give Eqs. (2) and (3), respectively.

$$r_{NO2-} = k_{\textbf{(absence of O2)}}[NO_2^-]^{0.3}P_{H2}^{0.4} \quad (2)$$

$$r_{NO2-} = k_{\textbf{(presence of O2)}}[NO_2^-]^{0.8}P_{H2}^{3.1} \quad (3)$$

In the absence of O_2, the reaction orders with respect to NO_2^- and H_2 were 0.3 and 0.4, respectively. It is presumable that NO_2^- and H_2 competitively adsorb on the Pt sites. Thus, the similar reaction orders with respect to NO_2^- and H_2 suggest that adsorbability of NO_2^- toward the Pt sites is comparable with that of H_2. As a result, the surface concentrations of both N_{ad} and H_{ad} are moderate, being at suitable levels for the formation of NH_3 under the reaction conditions of $\mathbf{NO_2^-–H_2}$.

On the other hand, both reaction orders became much larger in the presence of O_2 (0.8 and 3.1 for NO_2^- and H_2, respectively) than those in the absence of O_2. It is noted that the increase in the reaction order caused by the addition of O_2 was much more significant for H_2 than that for NO_2^-. This large reaction order with respect to H_2 (=3.1) cannot be explained with a common reaction model over catalysts. Comparison of the reaction rate for the hydrogenation

of NO_2^- (Fig. 1a) with that for the H_2O formation (Fig. 2) indicates that the latter was much faster than the former. This fact means that most of H_{ad} on the Pt surface were consumed for the H_2O formation in the presence of O_2 and thus the Pt surface had little H_{ad} under the reaction conditions of **NO_2^--H_2-O_2** (Scheme 2). Under this situation over the Pt sites, concentration of H_{ad} could steeply increase with increase in the partial pressure of H_2. We suppose that this leads to the unusually large reaction order with respect to H_2 in the presence of O_2.

It has been reported that the particle size of a precious metal has a big impact on the selectivity for the hydrogenation of NO_2^- in water. Yoshinaga *et al.*, have shown that the selectivity for NH_3 decreases with an increase in the size of Pd particles on active carbon and suggested that the NH_3 forms at the edge and corner sites of the Pd particles due to high hydrogenation-ability caused by the high coordination unsaturation.[28] In the present study, Pt/Al_2O_3 exhibited changes in the NH_3 selectivity similar to that over the Pd catalyst in **NO_2^--H_2**, that is, the selectivity for NH_3 decreased as the Pt particle size increased (Fig. 5). From the results, as is the case with the Pd catalyst, NH_3 formation may preferentially occur on the edge and corner sites of the Pt particles, whereas N_2 mainly forms on the terrace sites if there is no O_2 (Fig. 6(a)). Since the percentage of edge sites on the Pt particle with a diameter of 4.1 nm is calculated to be only 22% if the particle has cubo-octahedron shape,[29] the high selectivity for NH_3 in **NO_2^--H_2** indicates that the activities

of the edge and corner sites for the hydrogenation are much higher than that of the terrace sites.

In contrast, the selectivity for NH_3 did not depend on the Pt particle size for **NO_2^--H_2-O_2**. As was discussed before, H_{ad} on the Pt surface were mainly used by O_2 upon H_2O formation in the presence of O_2. Hence, the concentration of H_{ad} on the edge and corner sites of the Pt particle was naturally decreased. As a result, the edge and corner sites may be converted to the reaction sites active for N_2 formation owing to the suppression of H_{ad} concentration. In fact, the addition of O_2 increased the reaction rate for N_2 formation as demonstrated in Fig. 1. Therefore, we conclude that the inactivation of the edge and corner sites for the NH_3 formation and furthermore the change in the function of the sites from NH_3 formation to N_2 one in the presence of O_2 are the responsible for the high selectivity to N_2 over Pt/Al_2O_3 when O_2 is added to the H_2 stream (Fig. 6(b)), leading to the drastic changes in the selectivity.

Conclusions

Although Pt/Al_2O_3 gave NH_3 as a main product in the hydrogenation of NO_2^- with H_2 in water, the product drastically changed to N_2 when O_2 was added to the H_2 stream. Both the inactivation of the Pt sites active for the NH_3 formation and furthermore the change in

the function of the sites to form N_2 were the reasons for the high selectivity to N_2 over Pt/Al_2O_3 when O_2 is added to the H_2 stream. On the other hand, Pd/Al_2O_3 showed high selectivity for N_2 irrespective of the presence or absence of O_2, and Rh and Ru/Al_2O_3 were inactive for the hydrogenation of NO_2^- even in the absence of O_2. Our finding provides not only a new approach to achieve high selectivity in hydrogenation reactions but also provides valuable information for developing new catalysts.

Acknowledgements

This work was supported by JSPS KAKENHI Grant Number 15J05423 and 18H01780.

Conflicts of interest

There are no conflicts to declare.

References

1 H. Lindlar, *Helv. Chim. Acta*, 1952, **35**, 446–450.

2 P. Landon, P. J. Collier, A. J. Papworth, C. J. Kiely and G. J. Hutchings, *Chem. Commun.* 2002, 2058–2059.

3 J. Hirayama, I. Orlowski, S. Iqbal, M. Douthwaite, S. Ishikawa, P. J. Miedziak, J. K. Bartley, J. K. Edwards, Q. He, R. L. Jenkins, T. Murayama, C Reece, W. Ueda, D. J. Willock and G. J. Hutchings, *J. Phys. Chem. C*, 2019, **123**, 7879–7888.

4 T. Mitsudome, K. Miyagawa, Z. Maeno, T. Mizugaki, K. Jitsukawa, J. Yamasaki, Y. Kitagawa and K. Kaneda, *Angew. Chem. Int. Ed.*, 2017, **56**, 9381–9385.

5 K.-D. Vorlop and T. Tache, *Chem. Ing. Tech.*, 1989, **61**, 836–837.

6 K. D. Hurley and J. R. Shapley, *Environ. Sci. Technol.*, 2007, **41**, 2044–2049.

7 W. Gao, R. Jin, J. Chen, X. Guan, H. Zeng, F. Zhang, Z. Liu and N. Guan, *Catal. Lett.*, 2003, **91**, 25–30.

8 S. C. Paik and J. S. Chung, *Appl. Catal. B*, 1996, **8**, 267–279.

9 C. Barroo, S. V. Lambeets, F. Devred, T. D. Chau, N. Kruse, Y. De Decker and T. Visart de Bocarme´, *New J. Chem.*, 2014, **38**, 2090–2097.

10 C. Barroo, Y. De Decker and T. Visart de Bocarme´, *J. Phys. Chem. C*, 2017, **121**, 17235–17243.

11 T. J. Schwartz, S. M. Goodman, C. M. Osmundsen, E. Taarning, M. D. Mozuch, J. Gaskell, D. Cullen, P. J. Kersten and J. A. Dumesic, *ACS Catal.*, 2013, **3**, 2689–2693.

12 J. Hirayama and Y. Kamiya, *J. Catal.*, 2017, **348**, 306–313.

13 M. Orazov and M. E. Davis, *Proc. Natl. Acad. Sci. U. S. A.*, 2015, **112**, 11777–11782.

14 A. Corma, P. Serna, P. Concepcion and J. Juan Calvino, *J. Am. Chem. Soc.*, 2008, **130**, 8748–8753.

15 P. Liu and E. J. Hensen, *J. Am. Chem. Soc.*, 2013, **135**, 14032–14035.

16 W. Luo, M. Sankar, A. M. Beale, Q. He, C. J. Kiely, P. C. Bruijnincx and B. M. Weckhuysen, *Nat. Commun.*, 2015, **6**, 6540–6549.

17 M. Kim, Y. Su, A. Fukuoka, E. J. M. Hensen, K. Nakajima, *Angew. Chem. Int. Ed.*, 2018, **57**, 8235–8239.

18 L. Yumin, L. Shetian, Z. Kaizhentg, Y. Xingkai and W. Yue, *Appl. Catal. A*, 1998, **169**, 127–135.

19 E. K. Hanrieder, A. Jentys and J. A. Lercher, *ACS Catal.*, 2015, **5**, 5776–5786.

20 M.-M. Pohl, J. Radnik, M. Schneider, U. Bentrup, D. Linke, A. Brückner and E. Ferguson,

J. Catal., 2009, **262**, 314–323.

21 E. K. Hanrieder, A. Jentys and J. A. Lercher, *Catal. Sci. Technol.*, 2016, **6**, 7203–7211.

22 A.C. Sunil Sekhar, A. Zaki, S. Troncea, S. Casale, C.P. Vinod, J.P. Dacquin, P. Granger, *Appl. Catal. A*, 2018, **564**, 26–32.

23 U. Prüsse and K.-D. Vorlop, *J. Mol. Catal. A*, 2001, **173**, 313–328.

24 R. Zhang, D. Shuai, K. A. Guy, J. R. Shapley, T. J. Strathmann and C. J. Werth, *ChemCatChem*, 2013, **5**, 313–321.

25 J. Hirayama and Y. Kamiya, *ACS Catal.*, 2014, **4**, 2207–2215.

26 J. Hirayama and Y. Kamiya, *Catal. Sci. Technol.*, 2018, **8**, 4985–4993.

27 B. P. Chaplin, E. Roundy, K. A. Guy, J. R. Shapley and C. J. Werth, *Environ. Sci. Technol.*, 2006, **40**, 3075–3081.

28 Y. Yoshinaga, T. Akita, I. Mikami and T. Okuhara, *J. Catal.*, 2002, **207**, 37–45.

29 C. M. Zalitis, A. R. Kucernak, J. Sharman and E. Wright, J. Mater. Chem. A, 2017, 5, 23328–23338.

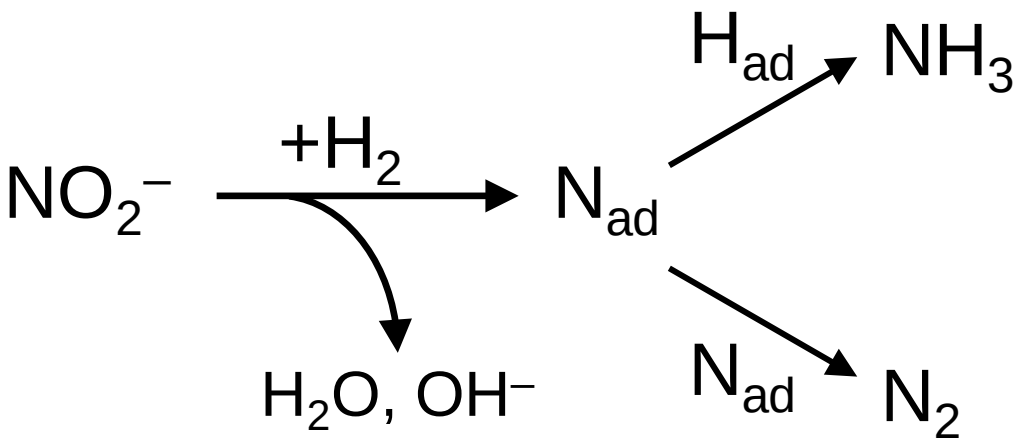

Scheme 1 Reaction pathway for catalytic hydrogenation of NO_2^- in water over precious metal catalysts.[23,24]

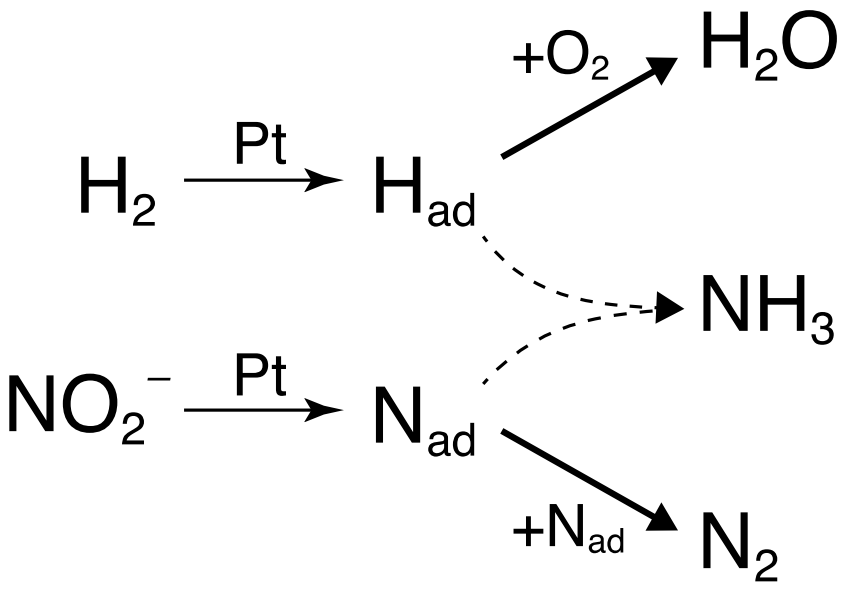

Scheme 2　Reaction pathway for catalytic hydrogenation of NO_2^- in the presence of O_2.

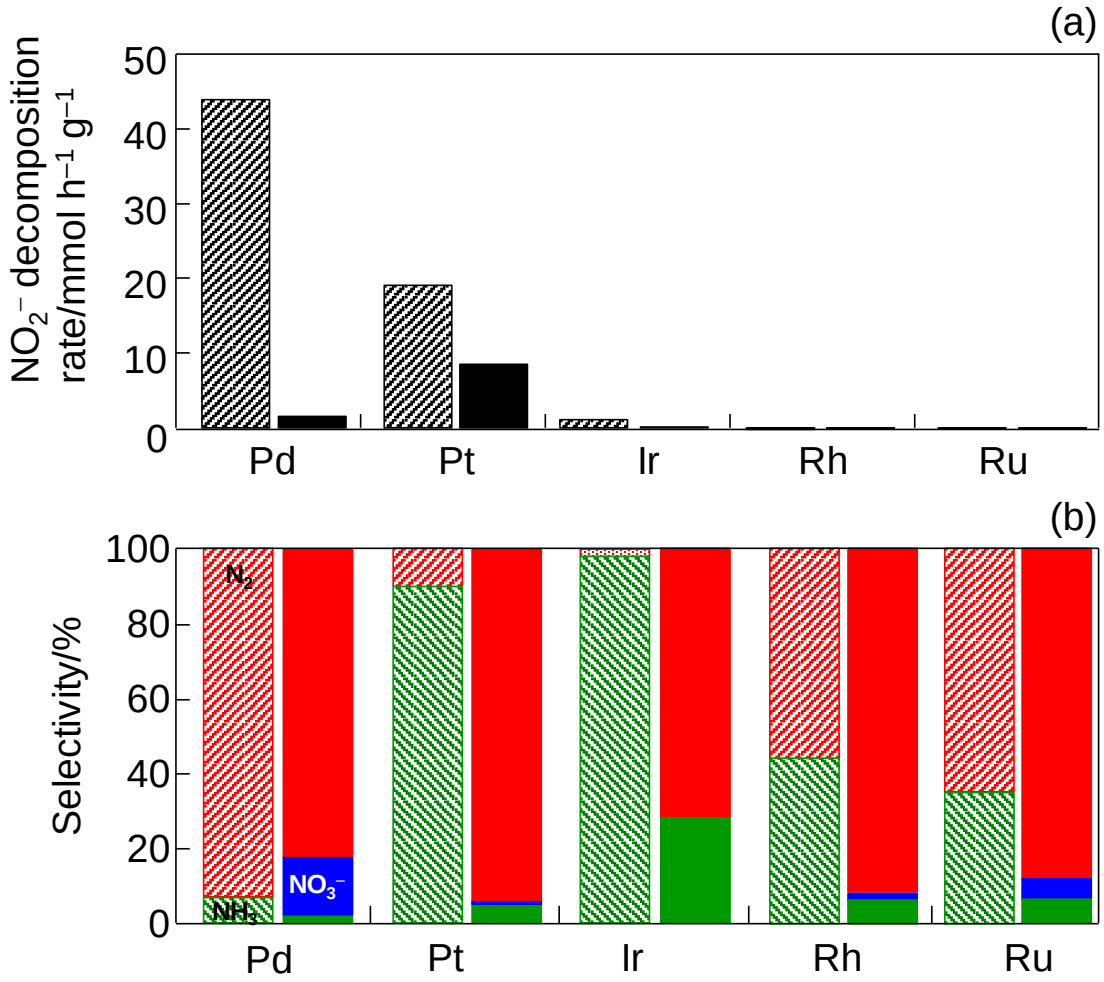

Figure 1 (a) NO_2^- decomposition rate and (b) selectivities for N_2 (red), NH_3 (green), and NO_3^- (blue) at 100% NO_2^- conversion for the catalytic hydrogenation of NO_2^- over M/Al_2O_3 (*M*: Pd, Pt, Ir, Rh, and Ru) in the absence (**NO_2^--H_2**) and presence (**NO_2^--H_2-O_2**) of O_2. Left (diagonal) and right (filled) bars represent the results for **NO_2^--H_2** and **NO_2^--H_2-O_2**, respectively. Reaction conditions: KNO_2, 1.0 mmol dm^{-3}; volume of reaction solution, 100 cm^3; total pressure, 1.0 atm; gas composition, H_2:CO_2:Ar = 2:3:5 (**NO_2^--H_2**) or H_2:CO_2:Ar:O_2 = 2:3:4:1 (**NO_2^--H_2-O_2**); gas flow rate, 100 cm^3 min^{-1}; and reaction temperature, 298 K.

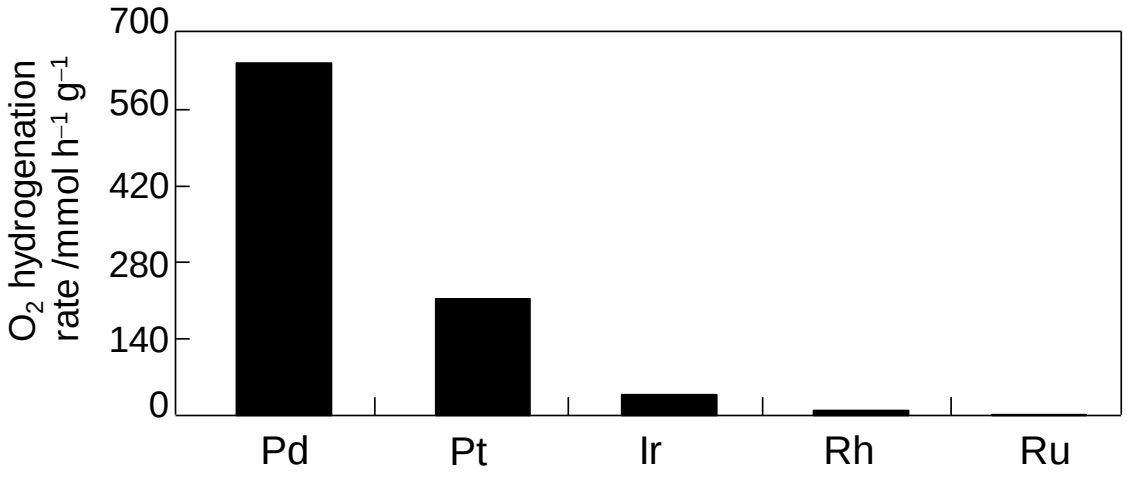

Figure 2 Reaction rate for O_2 hydrogenation in water over M/Al_2O_3 (M: Pd, Pt, Ir, Rh, and Ru). Reaction conditions: solvent, water; volume of water (without NO_2^-), 100 cm^3; total pressure, 1.0 atm; gas composition, H_2:O_2:CO_2:Ar = 2:1:3:4; gas flow rate, 100 cm^3 min^{-1}; and reaction temperature, 298 K.

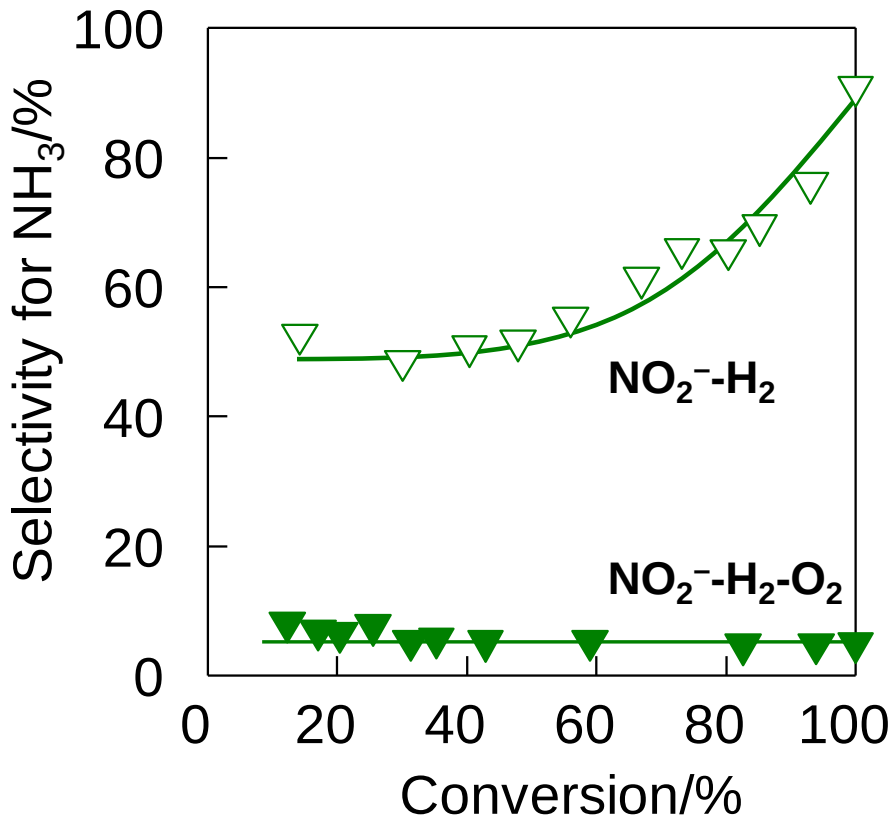

Figure 3 Dependence of the selectivity for NH_3 on NO_2^- conversion in the hydrogenation of NO_2^- over Pt/Al_2O_3. Reaction conditions: KNO_2, 1.0 mmol dm^{-3}; volume of reaction solution, 100 cm^3; total pressure, 1.0 atm; gas composition, H_2:CO_2:Ar = 2:3:5 (**NO_2^--H_2**) or H_2:CO_2:Ar:O_2 = 2:3:4:1 (**NO_2^--H_2-O_2**); gas flow rate, 100 cm^3 min^{-1}; and reaction temperature, 298 K.

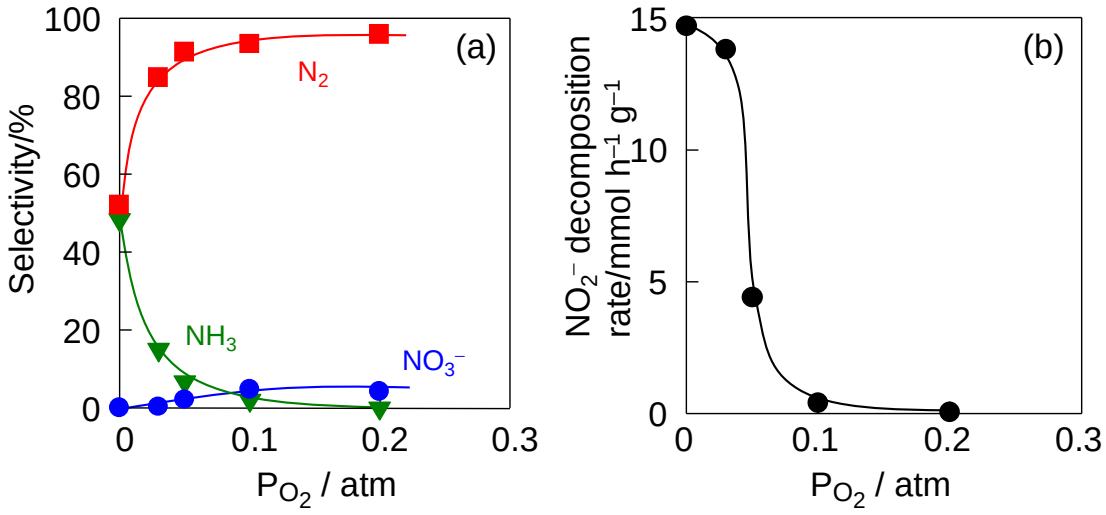

Figure 4 Influence of O_2 partial pressure on (a) selectivity and (b) NO_2^- decomposition rate for the catalytic hydrogenation of NO_2^- in water over Pt/Al_2O_3. Reaction conditions: KNO_2, 1.0 mmol dm^{-3}; volume of reaction solution, 100 cm^3; total pressure, 1.0 atm; gas composition, H_2:CO_2:Ar:O_2 = 1:3:6–4:0–2; gas flow rate, 100 cm^3 min^{-1}; and reaction temperature, 298 K.

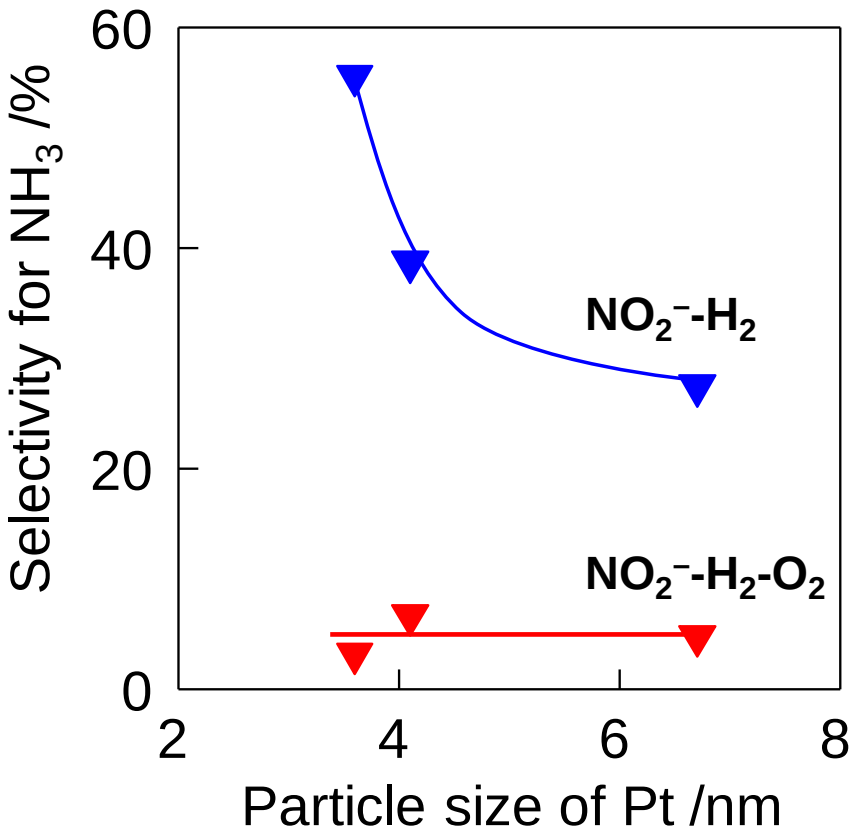

Figure 5 Effect of the Pt particle size on selectivity for NH_3 for the catalytic hydrogenation of NO_2^- over Pt/Al_2O_3 in the absence (**NO_2^--H_2**) and presence (**NO_2^--H_2-O_2**) of O_2. The particle sizes of Pt were estimated from CO chemisorption. Reaction conditions: KNO_2, 1.0 mmol dm^{-3}; volume of reaction solution, 100 cm^3; total pressure, 1.0 atm; gas composition, H_2:CO_2:Ar = 1:3:6 (**NO_2^--H_2**) or H_2:O_2:CO_2:Ar = 1:3:5:1 (**NO_2^--H_2-O_2**); gas flow rate, 100 cm^3 min^{-1}; and reaction temperature, 298 K.

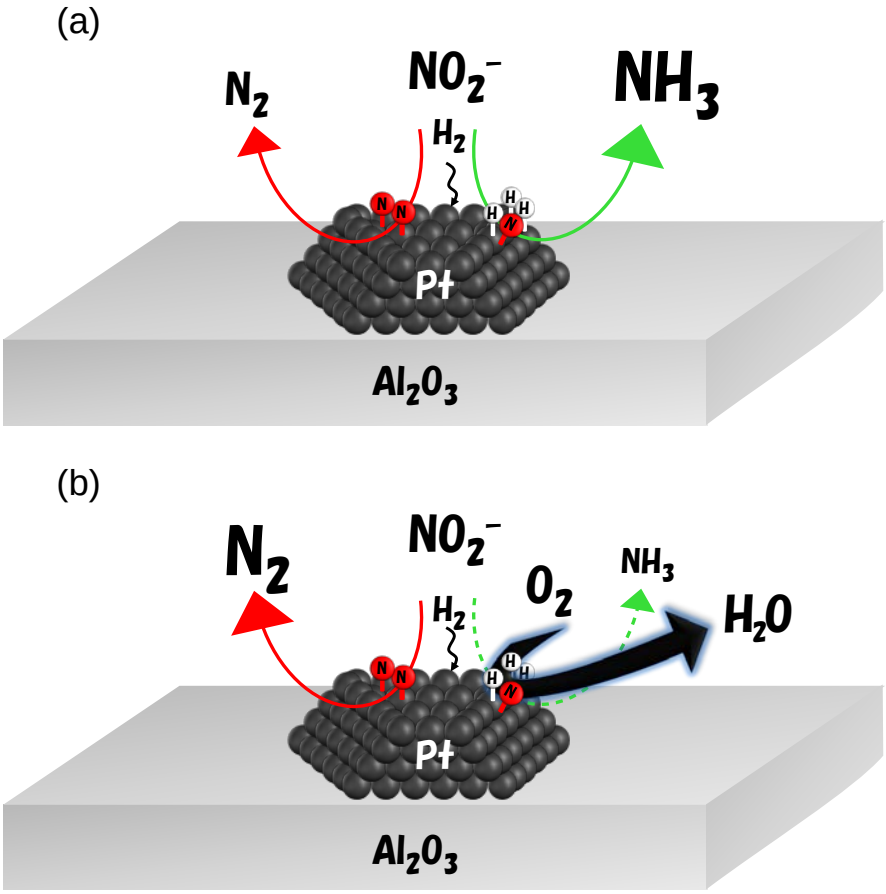

Figure 6 Proposed models for the hydrogenation of NO_2^- over Pt/Al_2O_3 (a) in the absence and (b) presence of O_2.